Dynamic Mapping of Diesel Engine through System identification

Henningsson, Maria; Ekholm, Kent; Strandh, Petter; Tunestål, Per; Johansson, Rolf

Published in:
Identification for Automotive Systems

DOI:
10.1007/978-1-4471-2221-0_13

2012

Chapter 13
Dynamic Mapping of Diesel Engine through System Identification*

Maria Henningsson**, Kent Ekholm, Petter Strandh,
Per Tunestål, and Rolf Johansson

Abstract. From a control design point of view, modern diesel engines are dynamic, nonlinear, MIMO systems. This paper presents a method to find low-complexity black-box dynamic models suitable for model predictive control (MPC) of NO_x and soot emissions based on on-line emissions measurements.

A four-input-five-output representation of the engine is considered, with fuel injection timing, fuel injection duration, exhaust gas recirculation (EGR) and variable geometry turbo (VGT) valve positions as inputs, and indicated mean effective pressure, combustion phasing, peak pressure derivative, NO_x emissions, and soot emissions as outputs. Experimental data were collected on a six-cylinder heavy-duty engine at 30 operating points. The identification procedure starts by identifying local linear models at each operating point. To reduce the number of dynamic models necessary to describe the engine dynamics, Wiener models are introduced and a clustering algorithm is proposed. A resulting set of two to five dynamic models is shown to be able to predict all outputs at all operating points with good accuracy.

13.1 Introduction

The heavy-duty engine market is dominated by compression-ignition diesel engines, due to their high energy conversion efficiency. Traditionally, this high

Maria Henningsson · Rolf Johansson
Department of Automatic Control, Lund University

Kent Ekholm · Per Tunestål
Department of Energy Sciences, Lund University

Petter Strandh
Volvo Powertrain Corp.
e-mail: maria.henningsson@control.lth.se.

* This work was supported by Vinnova and Volvo Powertrain Corp.

** Corresponding author.

D. Alberer et al. (Eds.): Identification for Automotive Systems, LNCIS 418, pp. 223–239.
springerlink.com

efficiency has come at the price of high levels of nitrogen oxides (NO_x) and soot particle emissions.

In the last decade, the emissions legislation has been dramatically tightened which has pushed for a shift in technology, either through introducing an aftertreatment system for NO_x reduction or through in-cylinder techniques. In the latter case, the combustion process is cooled down using a lower compression ratio, high levels of exhaust gas recirculation (EGR), and suitably chosen fuel injection timings resulting in so called Low Temperature Combustion (LTC) [7].

Control is a key factor for successful LTC diesel engines. One reason is that slow dynamics involved in e.g. EGR flow and cylinder wall temperature play a more important role when ignition delays are prolonged. Another reason is that tight requirements both in terms of emissions legislation and fuel economy make error margins tight. Diesel engine control design is normally based on a mix of physical mean-value models and experimental maps specifying optimal operating points in terms of emissions and fuel efficiency [1]. Feedback control uses indirect measurements such as manifold pressures and gas flows.

New sensor technology makes additional information from the combustion process available. Recently, NO_x sensors have been introduced in production engines giving the opportunity to adjust actuator settings according to measured emissions instead of precalibrated maps. These developments open up for e.g. model predictive control (MPC) that explicitly handles emission trade-off optimization based on on-line measurements of emissions. To that purpose, low-complexity dynamic models of the engine that also include emission formation are needed, this objective being the purpose of the work presented in this paper. The approach has been to use black-box system identification.

The focus has been to use direct measured information on the interesting engine outputs instead of relying on indirect measurements combined with models and maps. Measurements from a NO_x sensor, an opacimeter, and in-cylinder pressure sensors are therefore used. Though not all of these sensors are used in today's production engines, one can expect that if the benefits are large enough, the technology will eventually be available.

Different actuators can be used to optimize emissions, e.g. EGR and variable geometry turbine (VGT) valve positions [9, 8], fuel injection parameters [2], variable valve actuation [15], or some combination of these [5]. In this paper, the combined effect of the most significant diesel engine actuators (EGR, VGT, injection timing, and injection duration) is examined. These actuators are standard in heavy-duty diesel engines today and are all essential for optimization of engine operation. It would be desirable also to include engine speed as an input to the model, but for practical constraints in the laboratory setup that was not possible in this work.

The paper is organized as follows. Section 13.2 presents the experimental equipment and Section 13.3 briefly describes the thoughts behind the choice

of engine outputs and the experiment design. Section 13.4 describes the identification procedure, starting with local linear models that are expanded to Wiener models. A clustering algorithm is proposed to reduce the number of dynamic models required to describe the engine dynamics. Section 13.5 evaluates the identified models. Finally, conclusions and directions for future work are presented in Section 13.7.

13.2 Experimental Equipment

The experiments were conducted on a six-cylinder turbo-charged heavy-duty diesel engine with a displaced volume of $V_D = 12\text{e-}3[m^3]$. The compression ratio of the engine was reduced to $r_c = 14.1$ to facilitate low-temperature combustion. The engine was equipped with unit injectors for diesel where fuel injection timings could be set individually for each cylinder, with a low-pressure exhaust gas recirculation (EGR) loop where the EGR rate could be adjusted by a valve in the exhaust pipe, and with a variable geometry turbo (VGT) where the turbocharging also could be adjusted by a valve.

All cylinders were equipped with piezo-electrical, water-cooled pressure transducers of type Kistler 7061B [12], with cylinder pressure data sampled every 0.2 crank angle degrees using a Microstar DAP 5400a/627 data acquisition board [13]. The control system was based on a standard PC running Linux enabling cycle-to-cycle control. Fuel injection timings were updated every engine cycle, and the setpoints for the valve positions were updated with a frequency of 10 Hz.

The pressure measurements p as a function of crank angle θ from the in-cylinder pressure sensors were used to compute indicated mean effective pressure y_{IMEP}, combustion phasing α_{50}, and maximum pressure derivative d_p. The indicated mean effective pressure is defined as

$$y_{\text{IMEP}} = \frac{1}{V_D} \int p dV, \tag{13.1}$$

where the integral is taken over an engine cycle, and the maximum pressure derivative as

$$d_p = \max_{\theta} \frac{dp}{d\theta} \tag{13.2}$$

From the cylinder pressure p, the heat release rate dQ is computed using the relation

$$\frac{dQ}{d\theta} = \frac{\gamma}{\gamma - 1} p(\theta) \frac{dV}{d\theta} + \frac{1}{\gamma - 1} V(\theta) \frac{dp}{d\theta} \tag{13.3}$$

for the apparent heat release rate based on a fixed ratio of specific heats [3]. From the heat release rate, α_{50} is defined as the crank angle degree where 50 % of the heat has been released,

$$\frac{Q(\alpha_{50})}{\max_\theta Q(\theta)} = 0.5 \tag{13.4}$$

Emissions of NO_x were measured using a Siemens VDO / NGK Smart NOx Sensor [14]. Soot emissions were measured using an opacimeter from SwRI measuring the percentage of light absorbed by the exhausts in the exhaust pipe.

13.3 Experiment Design

Four control variables act as inputs to the model:

- the crank angle of start of fuel injection u_{SOI}
- the fuel injection duration measured in crank angle degrees u_{FD}
- the position of the EGR valve u_{EGR}
- the position of the VGT vanes u_{VGT}

such that

$$u = \left(u_{\mathrm{SOI}}\ u_{\mathrm{FD}}\ u_{\mathrm{EGR}}\ u_{\mathrm{VGT}}\right)^T. \tag{13.5}$$

For the main part of the work, five model outputs were considered; the net indicated mean effective pressure y_{IMEP}, the crank angle degree of 50 % fuel burnt α_{50}, the peak cylinder pressure derivative over the cycle d_p, the nitrogen oxide concentration y_{NOx} and the opacity of the exhausts y_{op} giving a measure of soot concentration

$$y = \left(y_{\mathrm{IMEP}}\ \alpha_{50}\ d_p\ y_{\mathrm{NOx}}\ y_{\mathrm{op}}\right)^T. \tag{13.6}$$

The first three output variables were cylinder-individual. The last two outputs, y_{NOx} and y_{op} were common to all cylinders. These five outputs were chosen because they are all required in the model predictive control setup for which the model is intended to be used. The planned control design setup is to minimize y_{op} and y_{NOx}, to let y_{IMEP} follow a reference, to keep α_{50} at a setpoint corresponding to maximum brake torque, and to limit d_p to avoid combustion modes that may damage the engine.

Many alternative measured outputs could be considered. By including more measured outputs in the model, prediction of the original outputs to be used for control could be expected to improve when more information is available for prediction. An extended set of outputs was thus also considered, where intake manifold pressure p_{in} and ignition delay α_{ID} were added to the output vector,

$$y_{ext} = \left(y_{\mathrm{IMEP}}\ \alpha_{\mathrm{ID}}\ d_p\ y_{\mathrm{NOx}}\ y_{\mathrm{op}}\ p_{\mathrm{in}}\ \alpha_{50}\right)^T. \tag{13.7}$$

The ignition delay was defined as $\alpha_{\mathrm{ID}} = \alpha_{10} - u_{\mathrm{SOI}}$, the time measured in crank angle degrees from start of injection until 10 % of fuel was burnt.

The study is limited to low and medium load operating points, where the possible impact of low temperature combustion is the greatest and where the associated slow dynamics are most dominant. A fixed engine speed of 1200 rpm was chosen, the study could easily be expanded to multiple engine speeds using the same methodology. Three different loads were chosen, corresponding to $y_{\text{IMEP}} = \{4 \text{ bar}, 7 \text{ bar}, 10 \text{ bar}\}$. At each load three different values of start of injection u_{SOI} were chosen, and at each such value four points in the u_{EGR}-u_{VGT} plane were determined. A few initial steady-state maps were used to define suitable operating points in terms of emissions and brake efficiency. At each operating point suitable amplitudes for pseudo-random binary sequence (PRBS) signals were determined. The switching frequency of the PRBS signal was adjusted to the dynamic characteristics of each of the inputs (more frequent switching for the fuel injection variables u_{SOI} and u_{FD}, and less frequent for the gas flow variables u_{SOI} and u_{VGT}). In total, 30 operating points were defined: 6 at load $y_{\text{IMEP}} = 4$ bar, 12 at load $y_{\text{IMEP}} = 7$ bar, and 12 and $y_{\text{IMEP}} = 10$ bar. At $y_{\text{IMEP}} = 4$ bar, it was concluded that keeping the VGT valve fully open at $u_{\text{VGT}} = 100$ was optimal in terms of emissions and fuel economy, so there was no need for excitation of that input. An overview of the operating points is given in Table 13.1.

13.4 Identification Procedure

Data of length 2800 engine cycles were collected at each operating point. The sample period was one engine cycle. Constant offsets were removed. From each data set, two separate data sets each of length 1300 engine cycles were taken for identification and validation. To avoid any cross-correlation between the identification and validation data, they were separated by 200 engine cycles. It was concluded that offsets differed between the cylinders whereas the dynamics were similar, so models were only identified for cylinder 5 which was determined to be representative for all six cylinders. The outputs were scaled to obtain the same order of magnitude.

The identification procedure is divided into two parts. First, linear models are identified separately for each operating point. Then, the number of models needed are reduced by introducing Wiener models and performing a clustering algorithm.

13.4.1 Identification of Local Linear Models

Linear state space models for each operating point of the form

$$\begin{aligned} x_{k+1} &= Ax_k + Bu_k + Kw_k \\ y_k &= Cx_k + Du_k + w_k \end{aligned} \tag{13.8}$$

Table 13.1 Operating points

Op. point	y_{IMEP} (bar)	u_{SOI} (CAD)	u_{FD} (CAD)	u_{EGR} (%)	u_{VGT} (%)	*speed* (rpm)
1	4	−5	5.8	10	100	1200
2	4	−12	5.8	10	100	1200
3	4	−20	5.8	10	100	1200
4	4	−5	5.8	13	100	1200
5	4	−12	5.8	13	100	1200
6	4	−20	5.8	13	100	1200
7	7	−5	7.1	53	33.5	1200
8	7	−10	7.1	53	33.5	1200
9	7	−15	7.5	53	33.5	1200
10	7	−5	7.1	56	40	1200
11	7	−10	7.3	56	40	1200
12	7	−15	7.5	56	40	1200
13	7	−5	7.2	50	23	1200
14	7	−10	7.4	50	23	1200
15	7	−15	7.6	50	23	1200
16	7	−5	7.3	56	28	1200
17	7	−10	7.4	56	28	1200
18	7	−15	7.5	56	28	1200
19	10	−9	10.4	76	29	1200
20	10	−13	10.8	76	29	1200
21	10	−17	10.7	76	29	1200
22	10	−5	10.5	82	29	1200
23	10	−10	10.6	82	29	1200
24	10	−15	10.8	82	29	1200
25	10	−5	10.6	82	40	1200
26	10	−10	10.6	82	40	1200
27	10	−15	10.8	82	40	1200
28	10	−5	10.5	90	40	1200
29	10	−10	10.6	90	40	1200
30	10	−15	10.9	90	40	1200

where $x_k \in \mathbb{R}^n$, $u_k \in \mathbb{R}^r$, and $y_k \in \mathbb{R}^m$ were identifed using the `n4sid` algorithm of the System Identification Toolbox in Matlab. As validation criterion, variance accounted for (VAF) was used [4]. For output i, VAF is defined as

$$VAF(i) = 100\left(1 - \frac{\text{var}(y_i - \hat{y}_i)}{\text{var}(y_i)}\right) \tag{13.9}$$

where y_i is the measured output in the validation data, and $\hat{y}_i$ is the predicted output of the model. The VAF gives the percentage of the variance of the output that is described by the model.

Models of orders $n = 2$ to $n = 12$ were identified at each operating point. The mean VAF over the five outputs as a function of model order for 20-step prediction is shown in Figure 13.1.

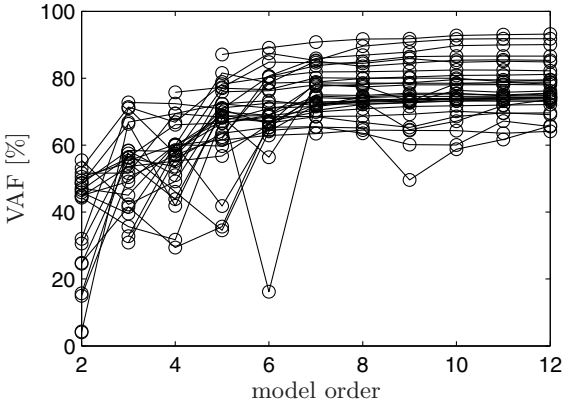

Fig. 13.1 VAF as a function of model order for the 30 operating points.

Low model orders, $n < 5$, lead to poor prediction. At some operating points, low-order models even lead to negative VAF (not included in Figure 13.1 for the sake of clarity) corresponding to a higher variance in the prediction error than in the measured outputs. Increasing the model order beyond $n = 7$ can give a small improvement in VAF, but not sufficient to motivate the greater computational burden of such large models for control design. From Figure 13.1, it can be concluded that model order $n = 7$ is suitable to describe the data. There is a large spread in VAF between the operating points for a fixed model order. This spread is mainly caused by different excitation of the outputs compared to the noise level at different operating points.

Figure 13.2 shows how VAF varies with prediction horizon for the five outputs for operating point 1.

13.4.2 Identification of Models for Extended Output Set

Models were also identified for the extended set of outputs in Eq. (13.7) and validated in terms of prediction of the original five outputs. Figure 13.3 shows the result for operating point 1. For low orders, the VAF for these models are significantly lower than for the original output set. This outcome could

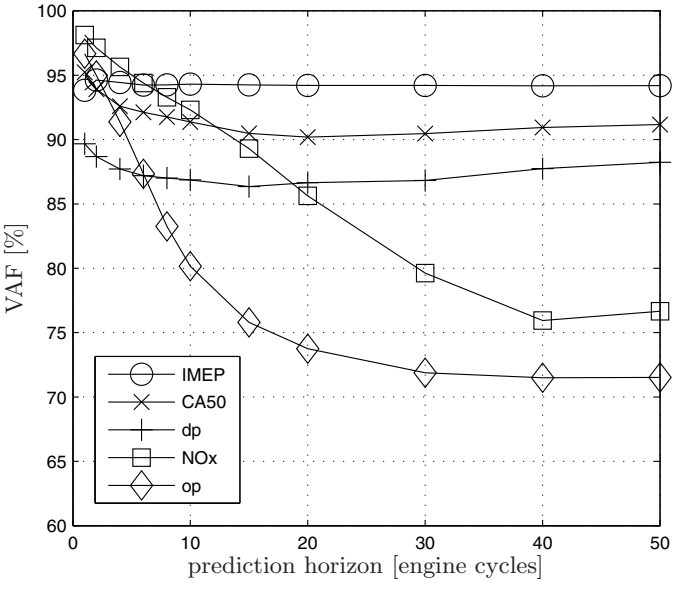

Fig. 13.2 VAF for different prediction horizons for the five outputs.

be expected, since with additional outputs the models need to incorporate additional dynamics particulary the slow intake manifold pressure evolution. At higher model orders, the VAF is similar for the original and the extended output set. It was thus concluded that there was not much to be gained from including the extra two outputs in the models and Kalman filter. In the following, only the original output set is considered.

13.4.3 Reducing the Number of Models

The purpose of the identification scheme is to find appropriate models for model-based control design. Since the process is clearly nonlinear, the controller must be based on more than one linear model leading to additional complexities of gain-scheduling and model-switching. With the computational resources available today, a feasible controller with cycle-to-cycle control in real-time cannot be based on 30 local linear models. Moreover, the models identified here are for a single engine speed and low-to-medium loads only. Expanding the mapping to cover the entire load-speed range of the engine, more models would have to be added.

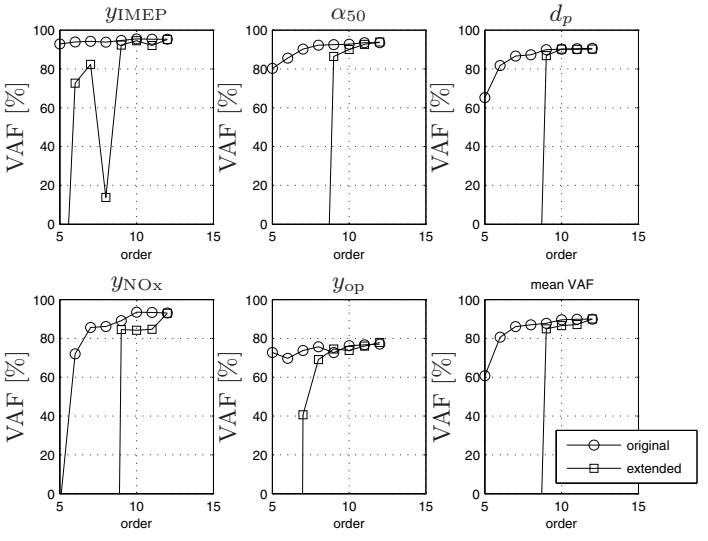

Fig. 13.3 VAF for 20-step prediction of models obtained for operating point 1 with the original and extended sets of outputs.

It is therefore of interest to see how close in behavior the models are to one another, i.e., if the same model could be used for more than one operating point. To that purpose, cross validation of all identified models to validation data at all operating points was performed. Figure 13.4 shows the resulting VAF for 20-step predictions.

It can be seen that, in general, the best model for data from an operating point is the model identified at that operating point, as would be expected. Some combinations of models and operating points give good predictions, others do not. Note that models identified at low load (operating points 1 to 6) cannot be used at higher loads since these models do not contain the u_{VGT} input, as described in Section 13.3.

Here, two steps are taken to find a limited number of dynamic models describing the data at all operating points. First, Wiener models are introduced to compensate for different gains at different operating points. A clustering algorithm is then applied to group the operating points and find a suitable model for each group.

13.4.3.1 Wiener Models

A powerful extension of linear models are the Wiener and Hammerstein model classes [4]. A Wiener model is a linear dynamic model in series with a static nonlinearity on the output, see Figure 13.5. A Hammerstein model is the

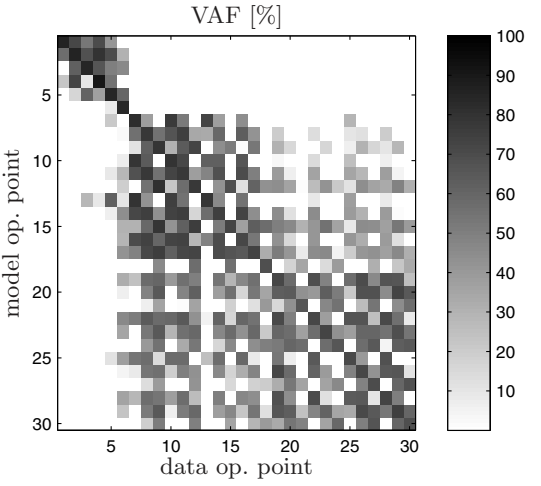

Fig. 13.4 Mean VAF for cross validation of the models identified at the 30 operating points with validation data at all operating points. Values on the diagonal are high, corresponding to good fit between model and data at the same operating point.

equivalent with the nonlinearity on the input. The static nonlinearity $f(\cdot)$ adds a large flexibility to the linear dynamic model at a moderate cost. If the nonlinearity can be inverted, control design can be based entirely on linear techniques. Here, we choose to use Wiener models rather than Hammerstein models because we have a 4-input-5-output system, which gives one more degree of freedom when transforming the output rather than the input. Previously, models of the form

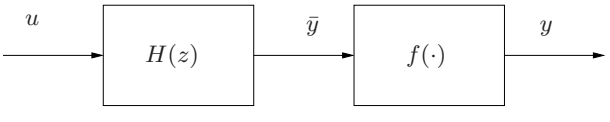

Fig. 13.5 A Wiener model consisting of a linear model $H(z)$ with a static nonlinearity on the output $f(\cdot)$.

$$x_{k+1} = A^i x_k + B^i u_k + K^i w_k$$
$$y_k = C^i x_k + D^i u_k + w_k,$$

where $x_k \in \mathbb{R}^n$, $u_k \in \mathbb{R}^r$, $y_k \in \mathbb{R}^m$, were identified for operating points $i = 1, \cdots, 30$. A Wiener model extends this representation to

$$
\begin{aligned}
x_{k+1} &= A^i x_k + B^i u_k + K^i w_k \\
\bar{y}_k &= C^i x_k + D^i u_k + w_k \\
y_k &= f^i(\bar{y}_k)
\end{aligned}
$$

Consider the dynamic model $\mathcal{M}_i(A^i, B^i, C^i, D^i, K^i)$ to be given from the previous identification procedure. We now wish to find a representation of the nonlinearities $f^i(\cdot)$ to let model i better fit data at another operating point j. This can be done through a local linearization of $f^i(\cdot)$ at operating point j,

$$
M^{ij} = \left. \frac{\partial f^i}{\partial \bar{y}} \right|_{\text{op point}=j} \tag{13.10}
$$

From the set of local linearizations M^{ij} and the offsets removed at each operating point, approximations of the nonlinearities $f^i(\cdot)$ can be reconstructed as e.g. piecewise linear functions.

We now wish to find the matrices M^{ij} to optimize the fit between model i and identification data j. To make the representation simpler and to avoid over-parameterization of the model, the matrices M^{ij} are constrained to be diagonal, $M^{ij} = \text{diag}(m_1^{ij}, \cdots m_m^{ij})$, such that the nonlinearity $f^i(\cdot)$ is decoupled into m scalar nonlinearities, one for each output.

Denote by $\hat{\bar{\mathcal{Y}}}_{ij} \in \mathbb{R}^{N \times m}$ the data series of predicted outputs at operating point j using model i with the nominal gain matrix $M^{ij} = I$. It then holds for the output data series of Wiener model $\hat{\mathcal{Y}}_{ij}$

$$
\hat{\mathcal{Y}}_{ij} = \hat{\bar{\mathcal{Y}}}_{ij} {M^{ij}}^T \tag{13.11}
$$

The optimal gains m_k^{ij}, $k = 1, \cdots, m$, can now be found by solving the convex optimization problems

$$
\min_{M^{ij} \text{ diagonal}} ||\mathcal{Y}_j - \hat{\bar{\mathcal{Y}}}_{ij} {M^{ij}}^T||_F^2 \tag{13.12}
$$

where $\mathcal{Y}_j$ is the measured output data series at operating point j.

The cross validation was redone with an optimized scaling matrix M^{ij} for each pair of model and data operating points i and j. The resulting VAF can be seen in Figure 13.6. Notice the large improvement in VAF when matching models to different operating points compared to Figure 13.4.

13.4.3.2 Model Clustering

From Figure 13.6, we can see that some of the linear models with adapted gains well describes data at many operating points. We define by V the VAF matrix illustrated in Figure 13.6, where element v_{ij} corresponds to the mean VAF over the five outputs when using Wiener model i for a 20-step prediction of validation data at operating point j. The matrix V can be used to group

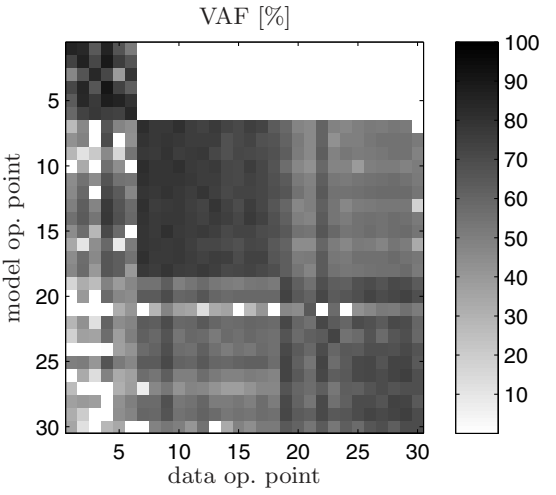

Fig. 13.6 Mean VAF for cross validation of the models identified at the 30 operating points with validation data at all operating points with gains adapted to form Wiener models. Note the large improvement compared to Figure 13.4.

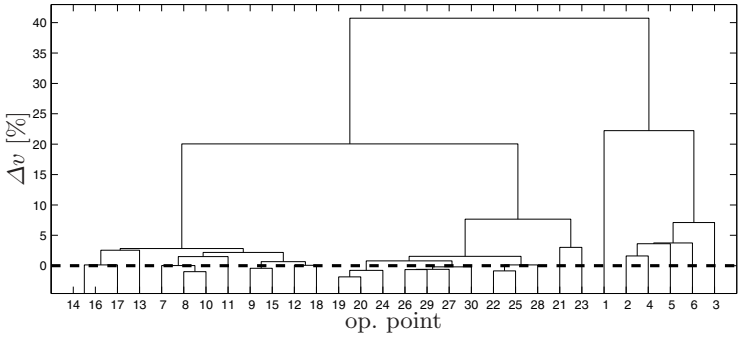

Fig. 13.7 Dendrogram of operating point clustering.

operating points to a limited number of models. A hierarchical agglomerative clustering algorithm is used to that respect [6].

The algorithm is based on the relative VAF loss matrix ΔV, where the elements are given by

$$\Delta v_{ij} = v_{jj} - v_{ij}, \tag{13.13}$$

and a clustering matrix C initialized as

$$C = \Delta V \tag{13.14}$$

The element Δv_{ij} is a measure of how much VAF that is lost by removing model j and using model i instead for that operating point. The hierarchical clustering algorithm successively merges two of the existing clusters at each step until only one cluster remains. At each step, the algorithm first finds the minimum element of C, corresponding to the smallest VAF loss, and merges models in cluster j into the cluster for model i. A new column is added to C representing the new cluster. The distance to other models for the newly formed cluster is defined as the worst-case distance over the included operating points to the model. The details of the algorithm are described in Algorithm 2.

Algorithm 2. Clustering algorithm based on the relative VAF loss matrix ΔV and the clustering matrix C.

Let $K =$ number of operating points.
Initialize $C = \Delta V$.
Set $\text{diag}(C) = \infty$ to mark that a cluster cannot merge with itself.
for $k = K + 1$ to $2K - 1$ **do**
    Find indices i, j of minimum element of C
    Merge cluster i and j into new cluster k, assign cluster i model to cluster k.
    Add a column to matrix C corresponding to cluster k, let $c_{\star k} = \max(\Delta v_{\star s_1}, \cdots, \Delta v_{\star s_L})$, where s_1 to s_L are the operating points previously assigned to clusters i and j, now to cluster k.
    Set $c_{\star k}$ to ∞ for models that have previously been removed.
    Remove clusters i and j by letting $c_{\star i} = \infty$, $c_{\star j} = \infty$.
    Remove cluster j model by letting $c_{model(j)\star} = \infty$.
end for

13.5 Identification Results

The result of the clustering procedure can be illustrated in a dendrogram, see Figure 13.7. The dendrogram shows the merges of operating points into clusters as a tree structure, starting at the bottom where every operating point is in its own cluster. On the y-axis, the loss of VAF is shown for each merge. It can be seen that a few models may be removed at no loss at all, which means that a model identified at a different operating point proved to be marginally better than the corresponding model in some cases. This result is likely due to the choice of prediction horizon in the computation of VAF. A large number of models may be removed at a moderate cost; if a loss of 5 % is accepted only six clusters remain, if 10 % can be accepted only four clusters are needed.

It can be noted that the clusters are not randomly assembled. With only two clusters remaining, one consists of the low load operating points 1 to 6, and the other to the medium and high load operating points 7 to 30. The

medium-to-high load cluster is further divided at a lower level into one cluster for medium load operating points 7 to 18 and one for high load operating points 19 to 30.

If we settle for five clusters, corresponding to a VAF loss of 7.5%, the worst-case fit between model and operating point will occur for operating point 3 which has been assigned to model 5. Figure 13.8 shows the measured output validation data at operating point 3, the 20 step prediction using model 3, and the 20 step prediction using model 5 with the adapted Wiener gain for operating point 3. It can be concluded that prediction of all outputs is very good using model 3, and only slightly worse using the adapted model 5. It can be expected that model 5 with the adapted Wiener gain is accurate enough to be used for control design.

13.6 Discussion

In general, it can be concluded that prediction based on the identified local linear models was very good for all five outputs. Standard system identification algorithms were used to fit dynamical black-box model of moderate order to four-input-five-output data sets. Considering the complexity of the task, the results are surprisingly good. Furthermore, the Wiener modeling combined with the clustering algorithm reduces the number of dynamic models needed to an acceptable level while keeping the predictive ability of the remaining models high. The results are a promising start for model based control design that uses direct emissions measurements.

Alternative approaches to the Wiener gain approximation and clustering procedures could be taken. For larger freedom in fitting data and models at different operating points, non-diagonal Wiener gain matrices could be considered. Whereas no detailed analysis of non-diagonal structure vs. cluster complexity was done, we would expect that the increase of coefficients to estimate would deteriorate statistical properties and thus require more data. Other clustering techniques might also be considered, such as the Tagaki-Sugeno model structure [11].

The choice of measured variables to be included as model outputs is not evident. From the purpose of the study, it is clear that y_{IMEP}, y_{NOx}, and y_{op} need to be included. Besides reduced emissions, an important goal of diesel engine control is to minimize fuel consumption. In the test engine, fuel consumption measurements were slow and inexact, so they were not a viable choice of output. Since combustion phasing α_{50} is one important factor in determining the efficiency of the engine, it was included as an output to allow for some influence over brake efficiency in the control design. To limit audible noise and avoid damage to the engine, it is necessary to limit the peak pressure derivatives over the cycle d_p, which was thus included as an output.

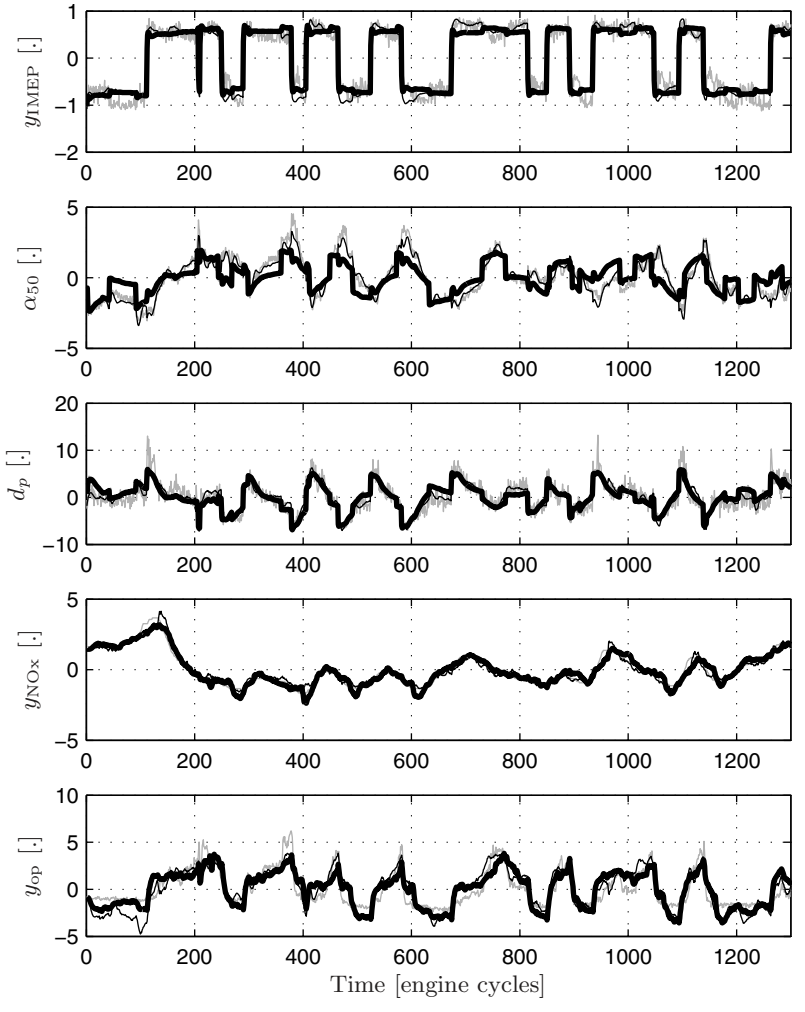

Fig. 13.8 Measured output of validation data at operating point 3 (gray solid line), 20-step ahead predicted output of local linear model identified at the same operating point (dashed line), 20-step ahead predicted output using model assigned through clustering algorithm (black solid line). The clustering algorithm was specified to set the level of accepted VAF loss at 7.5 %, yielding 5 dynamic models for the 30 operating points. Data are provided in scaled, arbitrary units.

Identification using the extended output vectors did not show any benefits by including intake manifold pressure and ignition delay as outputs to the models. These quantities are common in research on diesel engine combustion and intuitively one would expect that using information from these

additional measurements would result in better prediction. It is likely that the information could be of use if some other model structure were considered.

A common issue in system identification of control-oriented models of diesel engines is to handle the MIMO and nonlinear nature of the process. As more actuators are added to provide new degrees of freedom for optimizing emissions and fuel consumption, the experiment design and control design tasks suffer from the curse of dimensionality. The same is true for the approach suggested here. Expanding the study to cover the entire speed-load range of the engine and possibly also other inputs such as a second fuel injection would substantially increase the number of operating points required for identification.

Thus, new developments in actuator technology make the control design task harder. However, we could expect that this will to a certain extent be counteracted by new developments in sensor technology. With added on-line measurements of the important outputs, such as NO_x, the requirements on off-line calibration could be substantially reduced. A fine grid of pre-calibrated static maps could be replaced by a coarse grid of dynamic models. If done right, the total experimental effort required for developing the engine controller need not increase.

Physical modeling could be advocated in order to reduce experimental efforts. The results presented here could give some insights into the necessary structure of a physical model to be used for the purpose of on-line control of emissions. The authors are not aware of a practical physical model of moderate order with the chosen set of inputs and outputs. It would be interesting to pursue work in that direction, and to see a discussion of what physical quantities that best represent the 7 states needed for prediction.

A number of approaches to model MIMO, nonlinear dynamics of the diesel engine presented in the literature use neural networks [2, 10, 8]. In contrast to these works, the procedure presented here produces models on state-space form including noise models that fits directly into the framework of common control design methodologies such as MPC and LQG. State-space models are convenient for MIMO processes since they provide a compact representation of the response in all inputs and outputs and only one order needs to be chosen for all inputs and outputs.

13.7 Conclusions

A method to model diesel engine dynamics over a range of operating points using system identification was presented. The model captures the influence of the most significant actuators on a set of important engine outputs. Notably, the model can predict measured emissions very well. For future work, it will be of interest to see what can be achieved using direct closed-loop control of measured emissions instead of indirect control through other measured variables which has been the dominant approach hitherto.

Acknowledgement

The authors would like to thank T. Henningsson for helpful suggestions on optimization of Wiener gain matrices.

References

[1] Guzzella, L., Onder, C.H.: Introduction to Modeling and Control of Internal Combustion Engine Systems. Springer, Berlin (2004)
[2] Hafner, M., Schüler, M., Nelles, O., Isermann, R.: Fast neural networks for diesel engine control design. Control Engineering Practice 8(11), 1211–1221 (2000)
[3] Heywood, J.B.: Internal Combustion Engine Fundamentals. McGraw-Hill, New York (1988)
[4] Johansson, R.: System Modeling and Identification. Prentice-Hall, Englewood Cliffs (1993)
[5] Karlsson, M., Ekholm, K., Strandh, P., Johansson, R., Tunestål, P.: LQG control for minimization of emissions in a diesel engine. In: Proc. of the IEEE Multi-Conference on Systems and Control, San Antonio, TX, USA, pp. 245–250 (2008)
[6] Manning, C.D., Raghavan, P., Schütze, H.: Introduction to Information Retrieval. Cambridge University Press, Cambridge (2008)
[7] Musculus, M.P.B.: Multiple simultaneous optical diagnostic imaging of early-injection low-temperature combustion in a heavy-duty diesel engine. SAE Technical Paper 2006-01-0079 (2006)
[8] Omran, R., Younes, R., Champoussin, J.C.: Optimal control of a variable geometry turbocharged diesel engine using neural networks: Applications on the ETC test cycle. IEEE Transactions on Control Systems Technology 17(2), 380–393 (2009)
[9] Ortner, P., del Re, L.: Predictive control of a diesel engine air path. IEEE Transactions on Control Systems Technology 15(3), 449–456 (2007)
[10] Schreiber, A., Isermann, R.: Identification methods for experimental nonlinear modeling of combustion engines. In: Proc. for the Fifth IFAC Symposium on Advances in Automotive Control, Aptos, CA, pp. 351–357 (2007)
[11] Takagi, T., Sugeno, M.: Fuzzy identification of systems and its application to modeling and control. IEEE Transactions on System Man and Cybernetics 15(1), 116–132 (1985)
[12] `http://www.kistler.com`
[13] `http://www.mstarlabs.com`
[14] `http://www.vdo.com`
[15] Yilmaz, H., Stefanopoulou, A.: Control of charge dilution in turbocharged diesel engines via exhaust valve timing. In: Proc. American Control Conference, pp. 761–766 (2003)